Kinetics of oxidation of pure iron near the eutectoid temperature of Wüstite

K. GEMMA, M. KAWAKAMI, C. KOBAYASHI, N. ITOH, M. TOMIDA
Department of Materials Science, Tokai University, Kitakaname, Hiratuka, Japan

Kinetics of oxidation of pure iron near the eutectoid temperature of wüstite was investigated in atmospheric oxygen, and the reduction in the temperature dependence of the growth rate of iron oxides layer was examined. The results show a good agreement with those obtained from the linear theory of reaction rates in irreversible thermodynamics and the theory of absolute reaction rates.

1. Introduction

The oxidation of iron and steels (an important problem on steel making industry), has been investigated by a large number of investigators. As early as 1935, the phenomena of oxidation and scaling of iron and steels were studied and reviewed in detail [1]. Later, many studies of the kinetics and mechanism of oxidation of pure iron were carried out in greater detail and with more accuracy.

Gulbransen and Luka [2] investigated the reversible transormation of iron oxides, $Fe_3O_4 + Fe = 4FeO$, by the electron diffraction of films formed on pure iron at or near 843 K under low oxygen pressure. According to their results, both forward and reverse reactions occur in the oxides on slow cyclic heating and cooling of the specimens [2].

Davies *et al.* investigated the oxidation rate of pure iron and its mechanism in the temperature range 723 to 1223 K at atmospheric pressure in dry oxygen. Using a radio active tracer method, they found that 80% of the growth of magnetite on Wüstite depended on the diffusion of oxygen ions (O^{2-}) [3].

Paidassi and Fuller [4] also investigated the kinetics of oxidation of pure iron prepared under very careful pretreatment, e.g. heated in pure hydrogen at 1153 to 1273 K for 24 h, in the temperature range 673 to 973 K in atmospheric air [4]. They reported that for the logarithm of the isothermal constant, k against $1/T$, the Arrhenius plot of k shows a linear behaviour between 673 and 873 K even though the eutectoid temperature of wüstite lies in this range.

Caule *et al.* [5] measured the mass of Fe_2O_3 and Fe_3O_4 separately formed on pure iron oxidized in the temperature range 533 to 743 K in a low pressure of oxygen by an electrolytic reduction method and gravimetry with a microbalance. In their results, the Arrhenius plot of k is shown as linear in the experimental temperature range [5]. Thus, most results of investigations of the kinetics of oxidation of iron show that the Arrhenius plot of k is linear below the eutectoid temperature of wüstite ($T_{wüs}$).

Kubaschewski and Hopkins [6] collected both the results reported by Davies *et al.* [3] and by Schmahl *et al.* [7] into one figure as shown in Fig. 1. In Fig. 1, the relation between the logarithm of the rate constant, k_p ($g^2 cm^{-4} sec^{-1}$), and the reciprocal of absolute temperature below $T_{wüs}$, is drawn as a straight line. The figure is well known and is commonly recognized. From this historical background of the investigation of the kinetics of oxidation of iron, no significant problems are immediately recognized in Fig. 1. However, careful observation reveals that the loci of both experimental plots below about 840 K in this figure show a non-linear slightly convex.curve. We consider that these experimental plots below $T_{wüs}$ in Fig. 1 are correct from the similar non-linear phenomenon observed in the nitriding of austenitic stainless steel [8]. Thus the present investigation was undertaken to re-examine the kinetics of oxidation of pure iron below $T_{wüs}$. The growth kinetics of the magnetite layer formed on pure iron is discussed on the basis of a schematic free-energy diagram and using the linear theory of thermodynamics in irreversible processes.

2. Experimental details
2.1. Preperation of specimens
The electrolytic iron block (Atomiron M1, Syowa Denko Co. Ltd) containing impurities (mass %) C 0.0029; S 0.0036; P < 0.004; Si < 0.005; Mn < 0.005; Cu < 0.004; N 0.0016; O 0.047, as-received was first annealed at 1223 K in a hydrogen gas atmosphere. The annealed iron was then cold rolled. An iron sheet, 1 mm thick, was obtained. Pieces 10 mm × 10 mm were cut from the sheet, which were then decarburized at 1123 K for 3.6 k sec in a reducing atmosphere of H_2-H_2O gas mixture. The specimens used were prepared from these pieces after hand grinding using metallographic polishing paper (no. 1000), degreasing by wiping with a cloth dipped in trichloroethane, washing with this solvent in a glass beaker and with vapour of this solvent in a hot flask and drying. These were stored in a desiccator.
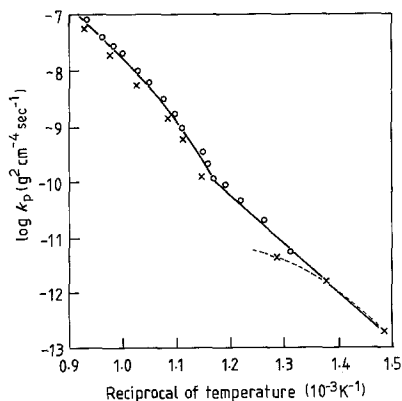
Figure 1 Relation between rate-constant and temperature for the oxidation of high-purity iron. (x) Davies *et al.* [3]; (O) Schmahl *et al.* [7].

2.2. Experimental methods

All specimens were pretreated in a supersonic bath with pure acetone before oxidation. The oxidation of specimens was carried out in a quartz reaction tube loaded in a vertical electric furnace in the temperature range 773 to 878 K for 1.5 to 54.0 k sec. The experiment was performed as follows. The electric furnace, which pre-held at a constant temperature by applying a steady electric current ready for oxidation, is first lowered to the bottom of the reaction tube. A specimen, previously weighed on a chemical balance, was loaded in the tube, then high purity oxygen gas was introduced from commercial cylinder through a flow-meter. After the air was purged, the furnace was raised to a fixed position, then the specimen was oxidized for a measured time, and cooled by again lowering the furnace. The furnace temperature was controlled using an automatic thermo-controller during oxidation of the specimen. The temperature of the specimen was measured using a calibrated chromel–alumel thermocouple beside the specimen. The oxidized specimen was reweighed and the thickness of the oxidized layer formed was measured by optical microscopy.

3. Results

Fig. 2 shows an optical microphotograph of specimens oxidized at 838 K for 6.0 k sec. Oxide layers were
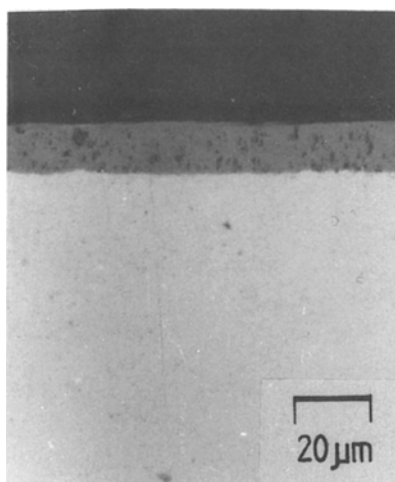

Figure 2 Optical micrograph of pure iron oxidized at 838 K for 6.0 k sec.
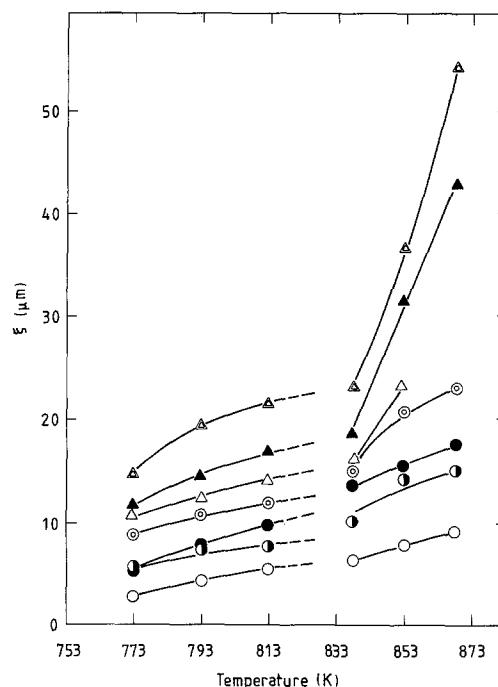

Figure 3 Thickness of oxide layers formed on pure iron in the temperature range 773 to 868 K for 1.5 to 54.0 k sec in oxygen at atmospheric pressure. Oxidizing time (k sec): (O) 1.5, (◑) 3.6, (●) 6.0, (◉) 13.5, (△) 24.0, (▲) 37.5, (▲) 54.0.

formed in close proximity with the base iron. Because the oxide metal boundary may be clearly observed, optical measurement of the thickness of oxide layer formed is easy. The thin haematite layer formed is not visible with the microscope. Fig. 3 shows average thickness (ξ) of the oxidized layer formed on the specimens plotted against oxidizing temperature in the range of 773 to 868 K for 1.5 to 54.0 k sec under atmospheric pressure of oxygen. A clear distinction in the growth rate of the oxidized layer is caused by the formation of wüstite in the oxide layer. In Fig. 3, two interesting phenomena are observed; first there is a decrease in the temperature dependence of the growth of the oxidized layer below 813 K, i.e. a reduction in the oxidation rate, and secondly the same tendency is observed above 833 K (at or near $T_{wüs}$) in the case of some treatment times. Only in the case of treatment in temperature range 833 to 868 K for 54.0 k sec does a general rate process, namely the Arrhenius law, seem to be obeyed. Fig. 4 shows the average mass increase (ΔW) of specimens oxidized plotted against temperature in the range 813 to 843 K for 6.0 k sec. It is seen that the temperature dependence of mass increase falls suddenly at 823 K, nearer to $T_{wüs}$. As the growth mechanism of oxide layers is a diffusion-controlled process with a chemical reaction, the lowering of both phenomena indicates a relationship between the diffusion process and the chemical reaction. This will be discussed later.

Fig. 5 shows the average thickness of the oxidized layer (ξ) plotted against the square root of oxidizing time ($t^{1/2}$). Although a few data in Fig. 5 are scattered, the growth of most oxide layers obeys a paraboric rate law without short-term oxidation below 833 K. The rate constants for the total thickness of the oxide layer or for mass increase (k' (m sec^{-1}) or k'' (g^2 m^{-4} sec^{-1}))
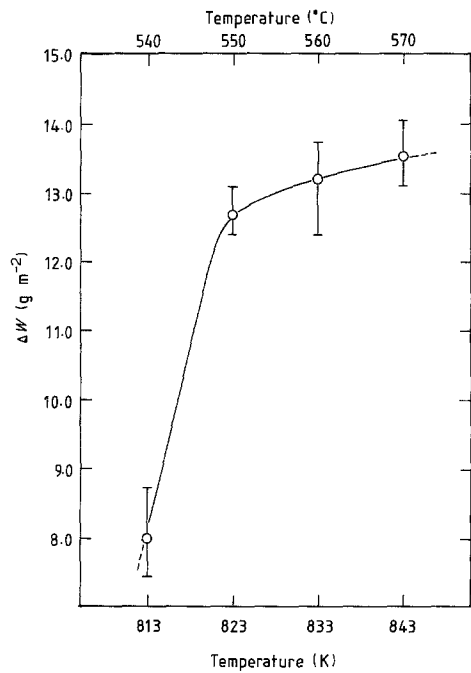
Figure 4 The retardation tendency of the oxidation rate of pure iron oxidized below and near the eutectoid temperature of wüstite for 6.0 k sec in oxygen at atmospheric pressure.

are then usually calculated from

$$\xi^2 = k't \tag{1}$$

$$\Delta W^2 = k''t \tag{2}$$

Equation 2 is used for results obtained by the gravimetric method. As the tangent of the linear function of Equation 1 gives k', a lowering of the rate below 838 K can be quantitatively shown in Fig. 5 by the decrease of tan k' with increasing temperature. A characteristic of the lowering tendency approaching $T_{\text{wüs}}$ can be shown by Arrehnius plots of the rate constant k'. The
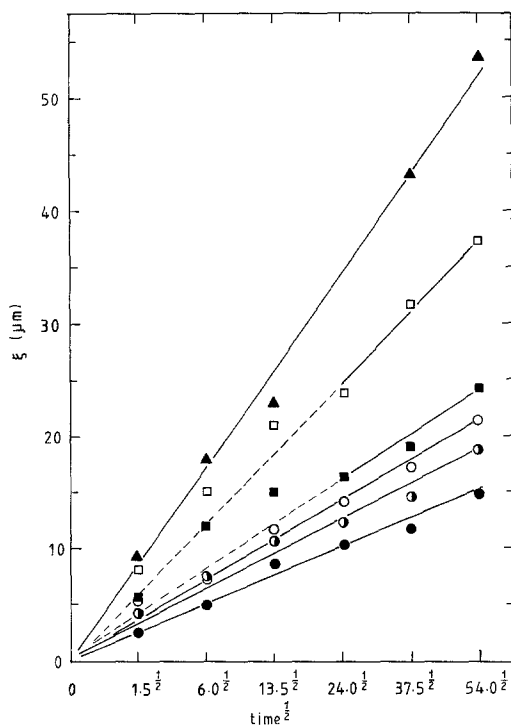

Figure 5 Thickness of the oxide layers plotted against the square root of time obtained from Fig. 3. (●) 773 K, (◑) 793 K, (○) 813 K, (■) 838 K, (□) 858 K, (▲) 878 K.
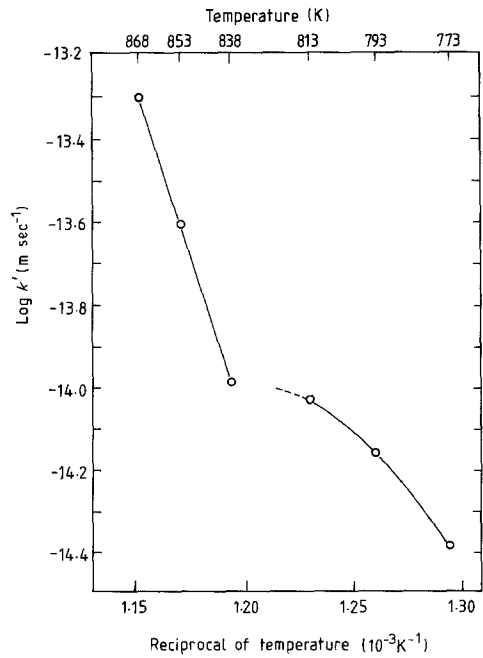

Figure 6 Plot of log rate constant in the growth of iron oxides layer against reciprocal of absolute temperature.

plot of log k' against the reciprocal of absolute temperature, is shown in Fig. 6. The equilibrium reaction at $T_{\text{wüs}}$ is given as $Fe_3O_4 + Fe = 4FeO$ [2]. Fig. 6 shows that the rate constant, k' approaches a constant value with temperature below about 838 K. Thus the forward and reverse reaction rates in the reaction $Fe_3O_4 + Fe = 4FeO$, reached equal-velocities at equilibrium temperature. A conception of the reaction rate at equilibrium may be introduced strictly in the theory of absolute reaction rates as presented by Glasstone *et al.* [9], thus the rate process near $T_{\text{wüs}}$ can be discussed on this basis. In addition, a conception of linear theory of the chemical reaction at near-equilibrium conditions in irreversible thermodynamics [10] will be available in understanding the lowering of the reaction near $T_{\text{wüs}}$, because this temperature is the thermodynamic critical point of the formation of both iron oxides of magnetite and Wüstite. At this temperature ($T_{\text{wüs}}$), the standard free energies of formation of these oxides have equivalent values, thus the reaction $Fe_3O_4 + Fe = 4FeO$ reaches equilibrium and the free energy of the reaction may be read from Equations 3 and 4 as shown later.

4. Discussion

4.1. Formation of the oxide layer

The structure of the oxide layer formed on pure metals is generally known from the diagram of the standard free energy of formation of oxides as a function of temperature, the T–$\Delta G°$ diagram. Fig. 7 shows a schematic T–$\Delta G°$ diagram for an iron–oxygen system adaped from Richardson and Jeffes [11, 12]. The dotted lines near 843 K represent metastable FeO (wüstite) and unstable Fe_3O_4 (magnetite). Present paper focuses on lowering of the oxidation rate below $T_{\text{wüs}}$ as shown in Fig. 7. Under conditions of 1 atm O_2 pressure below $T_{\text{wüs}}$, the structure of the oxide layer formed on pure iron consists of a duplex-layer of $Fe_2O_3/Fe_3O_4/Fe$, and these phases are in equilibrium at the Fe_2O_3/Fe_3O_4 and Fe_3O_4/Fe interfaces under a certain equilibrium
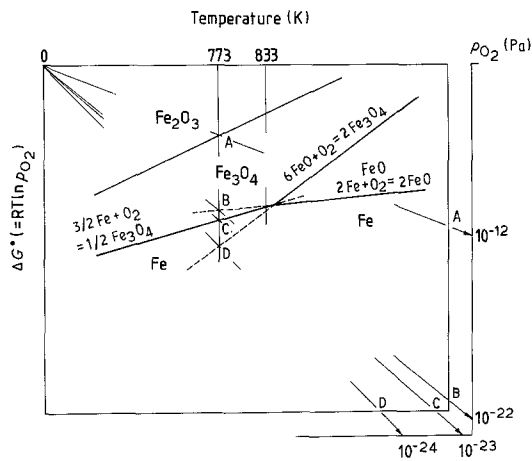
Figure 7 Schematic diagram of free energy of formation of iron oxides as a function of temperature [11, 12].

pressure of oxygen. According to the T-ΔG° diagram in Fig. 7, for example, 10^{-12} and 10^{-23} Pa oxygen pressure equilibriate approximately at the interfaces of Fe_2O_3/Fe_3O_4 and Fe_3O_4/Fe at 793 K, respectively. The growth of the Fe_2O_3 (haematite) layer is controlled by oxygen ions transported through the layer under a gradient of the chemical potential of oxygen corresponding 10^{-12} Pa from atmospheric pressure, because the magnetite layer formed beneath the haematite layer actually grows under a constant oxygen pressure of 10^{-12} Pa. The growth of the magnetite layer formed on Wüstite is found to be controlled by the transport of 80% oxygen ions and 20% iron ions [3]. It can be considered that the gradient of the chemical potential of oxygen in the layer controls mainly the diffusion of oxygen ions from the Fe_2O_3/Fe_3O_4 interface to that of Fe_3O_4/Fe. With a metastable state at the Fe_3O_4/Fe interface at 773 K near $T_{wüs}$, as shown in Fig. 7, the formation of a metastable FeO is possible in the layer near the interface. This fluctuating reaction will be related to ΔG° of the reaction $Fe_3O_4 + Fe = 4FeO$ as shown later.

According to the rates processes theory [3], the rate of the chemical reaction at equilibrium is determined from equilibrium between the reactants and products with a conjugated activated complex; for example, in the equilibrium of Equation 6, two equilibria exist simultaneously, i.e. the equilibria between the [Fe_3O_4 + Fe] system and an activated complex, and between this complex and the [4FeO] system. So the reaction rate (ω) near the equilibrium state is generally determined by the difference between a forward reaction rate ($\omega \rightarrow$) and a reverse rate ($\omega \leftarrow$). The growth of the magnetite layer is essentially a diffusion-

controlled process as well as a transference phenomenon of the metal–oxide interface, comparable to the growth of precipitates in alloys with simpler kinetics, because the rate of chemical reaction at the Fe_3O_4/Fe interface between oxygen ions and iron ions cannot be disregarded near $T_{wüs}$ as a kind of critical thermodynamic point. Because the transference rate of the interface is influenced by the driving force (free energy) in the system, it is considered that gradient of the chemical potential of oxygen formed in the magnetite layer is approximately kept constant under a restricted condition. An understanding of the chemical reaction at the interface of Fe_3O_4/Fe will then enable the experimental results to be explained correctly.

Fig. 8 shows a schematic free energy diagram for the formation of iron oxides under conditions of different temperatures, for example at 773 K, well below $T_{wüs}$, and at 833 K, just below $T_{wüs}$. The left-hand side shows the interface of Fe_2O_3/Fe_3O_4 with an equilibrium pressure of oxygen (π_{O_2}) of approximately 10^{-12} Pa. The reactants are shown as oxygen ions (O^{2-}) and iron ions (Fe^{2+}); the oxygen ions are diffused from the interface of Fe_2O_3/Fe_3O_4 and iron ions are dissociated from the base iron. Products show stable and unstable Fe_3O_4 and meta-stable FeO. The reactions for the formation of iron oxides with standard free energy are [11, 12].
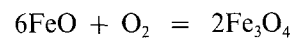
$$2Fe + O_2 = 2FeO$$
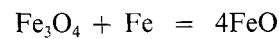$$\Delta G_4^\circ = -124\,100 + 29.90T \quad (3)$$
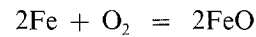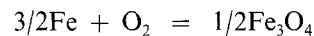
$$3/2Fe + O_2 = 1/2Fe_3O_4$$
$$\Delta G_5^\circ = -130\,390 + 37.37T \quad (4)$$

Then the following reactions with standard free energy may be read from the above equations

$$6FeO + O_2 = 2Fe_3O_4$$
$$\Delta G_6^\circ = -149\,240 + 59.80T \quad (5)$$

$$Fe_3O_4 + Fe = 4FeO$$
$$\Delta G_7^\circ = 12\,580 - 14.94T \quad (6)$$

The forward reaction in Fig. 8 has two probable ways in which to form metastable FeO and stable Fe_3O_4. Assuming free-energy hierarchy [14, 15], the formation of a metastable FeO is possible near $T_{wüs}$. When the metastable FeO is formed, this will behave as a reactant in the reverse reaction of Equation 3 with increasing local oxygen potential in the layer. The influence will counteract both the diffusion of oxygen ions and the formation of stable Fe_3O_4, based on

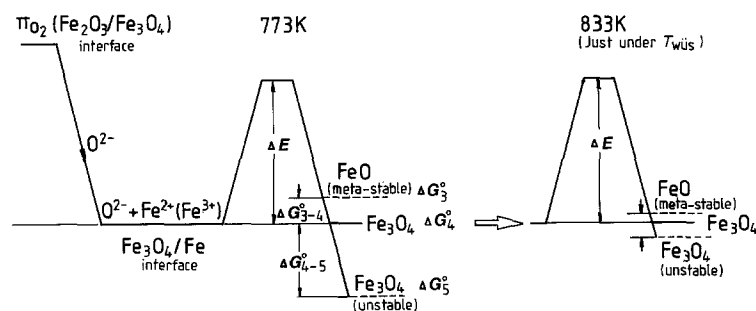*Figure 8* Schematic potential energy diagram for the formation of magnetite at Fe_3O_4/Fe interface below the eutectoid temperature of Wüstite. ΔG_{3-4}° and ΔG_{4-5}° show the difference between ΔG_3° and ΔG_4°, and ΔG_4° and ΔG_5°, respectively. ΔE denotes activation free energy of diffusion for iron ions in magnetite.

Equation 4, because the metastable FeO has a higher dissociation pressure of oxygen than Fe_3O_4 at the same temperature, as shown in Fig. 8. On the other hand, the metastable FeO formed may also be oxidized to unstable Fe_3O_4 under a certain oxygen potentials holding in the layer, Reaction 5. The equilibrium pressure of oxygen between magnetite and iron in Reaction 4 is higher than that of the pressure between magnetite and Wüstite in Reaction 5 at the same temperature. So, when unstable Fe_3O_4 is formed from the results of oxidation of the metastable Wüstite in the layer, this magnetite will immediately equilibrate with iron in accordance with Reaction 4. This suggests that the change in free energy of formation of the iron oxides at the Fe_3O_4/Fe interface affects the oxidation rate of iron below $T_{wüs}$. The kinetics of oxidation of pure iron has a complicated mechanism, as above mentioned; however, a thermodynamic interaction between the standard free energy of these oxides and temperature will explain the kinetics of decreasing of temperature dependence on the growth rate of the oxide layer observed in the experimental result.

Two assumptions are now made concerning the growth process of the oxidized layers: first, the diffusion rate of the oxygen ions in the magnetite layer is constant, because the equilibrium pressure of oxygen at both the Fe_2O_3/Fe_3O_4 and Fe_3O_4/Fe interfaces are virtually fixed in narrow temperature range, and second the rate of formation of iron oxides at the Fe_3O_4/Fe interface is rapid. In general, the rate of the chemical reaction is independent of the free energy (ΔG) well below the equilibrium state. However, near the critical thermodymanic point shown in Fig. 8, the rate of reaction is proportionly linear to affinity (A) on the basis of the theory or irreversible thermodynamics [10, 16].

4.2. Treatment on the basis of the thermodynamics of an irreversible process

The retardation tendency in the formation rate of iron oxides can be deduced from the linear theory of reaction rates based on irreversible thermodynamics [10]. For a general reaction A = B, the rate is usually given as $dB/dt = k^{\rightarrow}\alpha_A - k^{\leftarrow}\alpha_B$, where $k^{\rightarrow}$ and $k^{\leftarrow}$ are the rate constants of the forward and reverse reactions, respectively, α_A and α_B are the activities of components A and B. The above rate (ω) can be written as

$$\omega = k^{\rightarrow}\alpha_A [1 - (k^{\leftarrow}/k^{\rightarrow}) \alpha_B/\alpha_A] \qquad (7)$$

then the equilibrium constant (K) may be defined as

$$RT \log K = -(\nu_A \mu^{\circ}_A - \nu_B \mu^{\circ}_B)^* \qquad (8)$$

The affinity of the chemical reaction (A) is given by

$$A = RT \log K (\alpha_A/\alpha_B) \qquad (9)$$

$(k^{\leftarrow}/k^{\rightarrow})$ is usually employed as the equilibrium constant in the chemical kinetics, then Equation 7 is represented as follows

$$\omega = k^{\rightarrow}\alpha_A [1 - \exp(-A/RT)] \qquad (10)$$

*ν = stoichiometric coefficient, μ° = standard chemical potential.

Now consider the formation of Fe_3O_4 and FeO at the interface of Fe_3O_4/Fe; the two reaction rates, which are the rates of formation of Fe_3O_4 (ω_{mag}) and FeO $(\omega_{wüs})$, can be represented as

$$\omega_{mag} = \omega_0 [1 - \exp(-A_{mag}/RT)] \qquad (11)$$

$$\omega_{wüs} = \omega_0 [1 - \exp(-A_{wüs}/RT)] \qquad (12)$$

where ω_0 is the rate of the reactant system in Equations 3 and 4, because these reactions between iron ions and oxygen ions occur at the Fe_3O_4/Fe interface as shown in Fig. 8. A_{mag} and $A_{wüs}$ are the affinities of formation of magnetite and Wüstite, respectively. Well below $T_{wüs}$ there is no probability for the formation of wüstite, and thus the net reaction rate, ω_{net}, is determined by only ω_{mag} of Equation 12; but nearer $T_{wüs}$, the thermodynamic conditions at the Fe_3O_4/Fe interface reach a state where the probability of wüstite formation cannot be disregarded, and the net reaction must be influenced by $A_{wüs}$. It is expected that the rate of the net reaction will change as $A_{wüs}$ approaches A_{mag}. Then the net reaction rate can be written as

$$\omega_{net} = \omega_{mag} - \omega_{wüs}$$

$$= \omega_0 \exp(-A_{mag}/RT)$$

$$\times [\exp(A_{mag} - A_{wüs}/RT) - 1] \qquad (13)$$

From Equation 13, the change of ω_{net} in the oxidation rate of iron below and near $T_{wüs}$ may be represented semi-quantitatively, provided that the affinity is estimated in terms of the free energy function and ω_0 is replaced by the term $\kappa T/h$ in the equation presented in the theory of absolute reaction rates [9] where κ is Boltsmann's constant. ω_0 also represents the equilibrium rate in the linear theory of irreversible thermodynamics and this rate is the main concept of the theory of the absolute reaction rate.

Fig. 9 shows a relation between $\log \omega_{net}$ and reciprocal absolute temperature obtained from calculations with equation 13 by substituting ΔG°_5 and ΔG°_4 in A_{mag} and $A_{wüs}$, respectively. A clear agreement between the experimental and the theoretical results is shown here. Such a non-linear Arrhenius plot in the growth mechanism of layers as shown in Fig. 9 has not been published previously based on theory; however, Equations 10 and 15 imply fundamentally that the reaction rate near the critical thermodynamic point approaches limitlessly a fixed rate of equilibrium with change of ΔG° as a function of temperature.

In Equation 13 the term $\omega_0 \exp(-A_{mag}/RT)$ clearly represents the rate in the equilibrium state presented in the theory of absolute reaction rates shown in Equation 15, and the term $[\exp(A_{mag} - A_{wüs}/RT) - 1]$ is a factor which influences the rate of magnetite formation. The product of these terms, i.e. ω_{net}, appears in Fig. 9 as the sum of the logarithms of these terms. It is shown in Fig. 9 that the influence of $A_{wüs}$ for the net reaction begins from a limit of $2 \leqslant \exp(A_{mag} - A_{wüs}/RT)$. This restriction may give a general criterion for the reaction rate near the critical thermodynamic point.

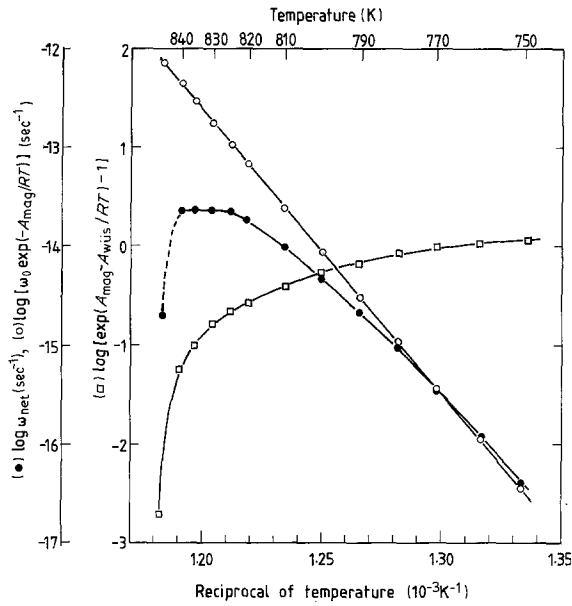Fig. 8 uses an explanation of kinetics in the theory

Figure 9 Reduction of the net oxidation rate of iron (ω_{net}) near the eutectoid temperature of Wüstite obtained by calculation using the linear theory of irreversible thermodynamics.

of absolute reaction rates [10], thus this theory will be dealt with briefly here. Taking an activation free energy of ΔE and a driving force of ΔG, the rate constant ($k^{\rightarrow}$) in the net reaction process is given by

$$k^{\rightarrow} = \kappa T/h \exp\left(-\Delta E/RT\right)\left[1 - \exp\left(-\Delta G/RT\right)\right]$$
(14)

where h is Planck's constant and R is the gas constant. When ΔG in Equation 15 takes a large enough value, and the reverse reaction rate may be disregarded, the net reaction depends only on ΔE.

Hume-Rothery [17] applied Equation 15 to explain the kinetics of precipitation in solids. The formation of magnetite at the Fe_3O_4/Fe interface is a kind of precipitation in a solid phase, and the growth rate of the oxidized layer of pure iron below $T_{wüs}$ may be analysed on the basis of Equation 14 using an analogous method reported previously.

Now it is considered that the formation of stable magnetite at the Fe_3O_4/Fe interface is determined by the reaction between oxygen ions (O^{2-}) diffusing from the surface and iron ions supplied from the base iron. In this process, the activation free energy of the reaction must be equivalent approximately to the activation free energy of diffusion of iron ions in magnetite. Iron ions must migrate in the magnetite phase because of its formation. In general cases, the activation energy of diffusion may be substituted for the activation free energy of diffusion (ΔE) presented in Equation 14. Taking 40.5 kcal mol^{-1} as the average activation energy in the kinetics of oxidation of pure iron to ΔE [18] in Equation 14, the tendency to reduce the oxidation rate of iron near $T_{wüs}$ can also be interpreted semi-quantitatively by the following equations for the formation of magnetite and Wüstite

$$k_{mag} = \kappa T/h \exp\left(-\Delta E/RT\right)\left[1 - \exp\left(-\Delta G^{\circ}_{mag}/RT\right)\right]$$
(15)

$$k_{wüs} = \kappa T/h \exp\left(-\Delta E/RT\right)\left[1 - \exp\left(-\Delta G^{\circ}_{wüs}/RT\right)\right]$$
(16)

then

$$k_{net} = k_{mag} - k_{wüs} = \kappa T/h \exp\left(-\Delta E/RT\right)$$
$$\times \exp\left(-\Delta G_{mag}/RT\right)$$
$$\times \left[\exp\left(\Delta G_{mag} - \Delta G_{wüs}\right)/RT - 1\right]$$
(17)

Equation 17 is comparable to Equation 13 introduced from the linear theory in the thermodynamics of irreversible processes. In Equation 17, the term $(\Delta G^{\circ}_{mag} - \Delta G^{\circ}_{wüs})$ is given directly on the T-ΔG° diagram, and the term $2 \leqslant \exp\left(\Delta G_{mag} - \Delta G_{wüs}\right)/RT$ gives a criterion here for lowering of the chemical reaction near the critical thermodynamic point. The term $\exp\left(-\Delta E/RT\right)$ for interstitial diffusion is contained in Equation 17 because this equation is applied for the reaction in a crystaloid solid; however, Equation 13, based on the reaction in a homogeneous system, does not contain this factor. Regardless of the fact that both equations are introduced on the basis of different theories they gave similar phenomenological confirmation of the experimental results obtained in this work.

Krichevskii *et al.* [19] reported a reduction in the reaction rate at the critical point for liquid–gas equilibrium in the $Cl_2 = 2Cl$ system on irradiation. Examination of the retardation of the chemical reaction rate near the critical thermodynamic points gave primary evidence for two concepts; first the equilibrium between reactants and an activated complex represented in the theory of absolute reaction rates, and second the determination of the rate of the net reaction by the difference between the forward rate and reverse rate.

Procaccia and Gittermann [20] offered a rule of thumb on the basis of a thermodynamic stability theory for understanding the critical slowing down of the chemical reaction. They also introduced the term $[(T - T_c)/T_c]^{\gamma}$ as a criterion at which the rates of reaction vanish. This term explains well the experimental results reported by Krichevskii *et al.* [19]; however, the term $\{[\exp\left(A_{mag} - A_{wüs}\right)/RT] - 1\}$, introduced based on the same theory, also explains the retardation phenomenon near critical thermodynamic point well in a heterogeneous system such as in the case of the oxidation of iron. The latter term consists of a function and factors confirmed by thermodynamic conceptions, and does not contain any infinitive factors such as the critical index, γ, in the former term, because the rate of reaction is explained directly and phenomenologically from Equations 13 and 17. However, the rates of reaction above and near $T_{wüs}$ have not been examined.

This work has some peculiarities in comparison with previous works [19, 20] as follows; (i) reaction in an open system as opposed to a closed system; (ii) reaction in heterogeneous solid phase as opposed to homogeneous phases, (iii) reaction under constant chemical potential as opposed to reduction by degrees. (iv) reaction under a steady state as opposed to a state approaching equilibrium.

It is also emphasized in this work that the rates of the processes between complicated chemical reactions must be treated, and the important result introduced

on the basis of both theories is examined comparatively easily regardless of the complicated reaction. The chromium–nitrogen system is a similar case to the iron–oxygen system on the T–ΔG° diagram. Two nitrides, Cr_2N and CrN, are formed in this system. The critical point of the chemical reaction to form these nitrides is found to be 703 K, approximately on the T–ΔG° diagram. In nitriding of the austenitic Fe–Cr–Ni alloy steel, lowering of the nitriding rate near the critical temperature is examined and reported [8]; however, examination using Equation 14 is not yet completed. Chemical reaction in solid phases, for example the oxidation of iron and the nitriding of the alloys, takes place with diffusion of ions or atoms. An interesting fact examined by experiments is that growth of oxidized and nitrided layers is restricted by the retardation of the chemical reaction near the critical temperatures. In these rate processes, the interaction between chemical reaction and diffusion is measurable, therefore detailed experimental and theoretical investigations are expected.

5. Conclusion

The rates of oxidation of pure iron in pure oxygen have been determined below the eutectoid temperature of Wüstite. These rates disagree with numerous results previously reported. Because the experimental results obtained showed that the temperature dependence of growth rates of the oxidized layer decreased slowly with temperature approaching $T_{w\ddot{u}s}$, the lowering of the rate of the chemical reaction near the critical temperature was examined, especially the reduction in mass increasing appearing remarkably just below $T_{w\ddot{u}s}$. This fact has not received much attention previously. A criterion for the estimation of the retardation of the reactions, $2 \leqslant \exp\left[(A_{mag} - A_{w\ddot{u}s})/RT\right]$, was offered a non-linear Arrhenius plot predicted, before the investigation was verified.

References

1. "Review of Oxidation and Scaling of Heated Solid Metals" (Department of Scientific and Industrial Research, London, 1935).
2. E. A. GULBRANSEN and R. RUKA, *J. Metals Trans. AIME* **188** (1950) 1500.
3. M. H. DAVIES, M. T. SIMNAD and C. E. BIRCHENALL, *J. Metals Trans. AIME* NY3 (1951) 889.
4. J. PAIDASSI and D. FULLER, *Bol. Soc. Chilena Quim.* **7** (1955) 26.
5. E. J. CAULE, H. BUOB and M, COHEN, *J. Electrochem. Soc.* **108** (1961) 829.
6. O. KUBASCHEWSKI and B. H. HOPKINS, "Oxidation of Metals and Alloys" (Butterworths, London, 1962) p. 109.
7. N. G. SCHMAHL, H. BAUMANN and H. SCHENCK, *Arch. Eisenhuttenw.* **207** (1956) 707.
8. K. GEMMA and M. KAWAKAMI, *J. Jpn Inst. Metals* **52** (1988) 701.
9. S. GLASSTONE, K. LAIDLER and H. EYRING, "The Theory of Rate Processes" (McGraw-Hill, New York, London, 1941).
10. P. GLANSDORFF and I. PRIGOGINE, "Thermodynamics Theory of Structure, Stability, and Fluctuations" (Wiley-Interscience, London, 1971), translated by G. Matsumoto and K. Takeyama. (Misuzu Shobo, Japan) p. 35.
11. F. D. RICHARDSON and J. H. E. JEFFES, *J. Iron Steel Inst.* **160** (1948) 261.
12. *Idem, ibid.* **163** (1949) 397.
13. K. RAIDLER, "Chemical Kinetics" (McGraw-Hill, London, 1965) p. 73.
14. W. OSTWALD, *Z. Phys. Chem.* **22** (1897) 289.
15. J. W. CHAN, "Rapid Solidification Processing, Principles and Technology II" (Claiter's, Baton Rouge, 1980) p. 24.
16. I. PRIGOGINE and R. DEFAY, "Thermodynamique Chimique" (Desoer, Liége, 1950), translated by M. Senoo. (Misuzu Shobo, Japan) p. 38.
17. W. HUME-ROTHERY, "The Structure of Alloys and Iron" (Pergamon Press, 1966), translated by K. Hirano (Kyouritu Shuppan, Japan) p. 142.
18. O. KUBASCHEWSKI and B. H. HOPKINS, "Oxidation of Metals and Alloys" (Butterworths, London, 1962) p. 111.
19. I. R. KRICHEVSKII, YU. V. TSEKHANSKAYA and Z. A. POLYAKOVA, *Russ. J. Phys. Chem.* **40** (1966) 715.
20. I. PROCACCIA and M. GITTERMANN, *Phys. Rev. Lett.* **46** (1981) 1163.